

Effect of substitution on the dimensionality of supramolecular aggregation in dihydrobenzopyrazoloquinolines

Jaime Portilla,^a Jairo Quiroga,^a Justo Cobo,^b John N. Low^c and Christopher Glidewell^{d,*}

^aGrupo de Investigación de Compuestos Heterocíclicos, Departamento de Química, Universidad de Valle, AA 25360 Cali, Colombia, ^bDepartamento de Química Inorgánica y Orgánica, Universidad de Jaén, 23071 Jaén, Spain, ^cDepartment of Chemistry, University of Aberdeen, Meston Walk, Old Aberdeen AB24 3UE, Scotland, and ^dSchool of Chemistry, University of St Andrews, Fife KY16 9ST, Scotland

Correspondence e-mail: cg@st-andrews.ac.uk

Received 21 June 2005

Accepted 24 June 2005

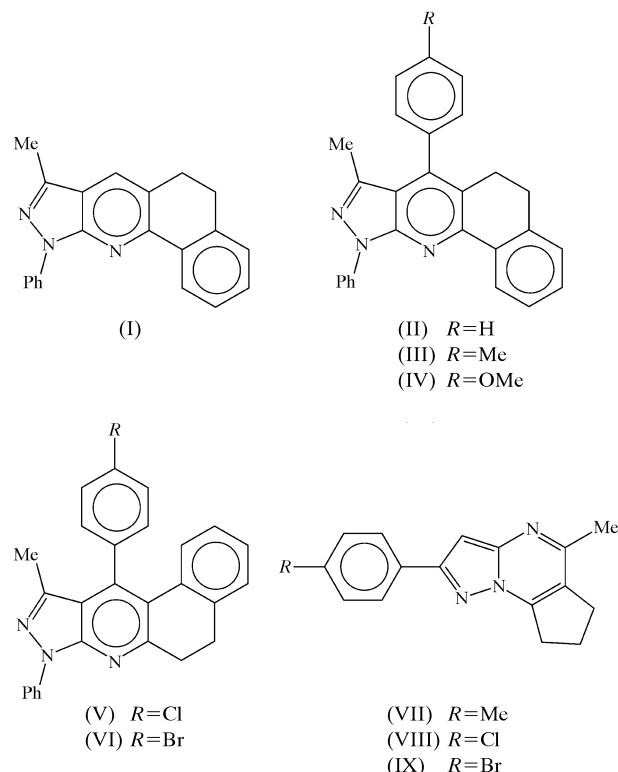
Online 23 July 2005

Molecules of 8-methyl-10-phenyl-6,10-dihydro-5*H*-benzo[*h*]pyrazolo[3,4-*b*]quinoline, C₂₁H₁₇N₃, (I), are linked into cyclic centrosymmetric dimers by means of paired C—H···N hydrogen bonds. In each of 8-methyl-7,10-diphenyl-6,10-dihydro-5*H*-benzo[*h*]pyrazolo[3,4-*b*]quinoline, C₂₇H₂₁N₃, (II), and 8-methyl-7-(4-methylphenyl)-10-phenyl-6,10-dihydro-5*H*-benzo[*h*]pyrazolo[3,4-*b*]quinoline, C₂₈H₂₃N₃, (III), the molecules are linked by C—H···π(arene) hydrogen bonds into sheets, although the detailed construction of the sheets is entirely different in (II) and (III). The molecules of 7-(4-methoxyphenyl)-8-methyl-10-phenyl-6,10-dihydro-5*H*-benzo[*h*]pyrazolo[3,4-*b*]quinoline, C₂₈H₂₃N₃O, (IV), are linked into a complex three-dimensional framework structure by a combination of C—H···N, C—H···O and three independent C—H···π(arene) hydrogen bonds.

Comment

Pyrazolo[3,4-*b*]quinolines are of interest as possible antiviral and antimalarial agents, and because of their other biological properties, such as parasiticidal, bactericidal, vasodilator, and enzyme-inhibitory activity (Quiroga *et al.*, 2001). We report here the structures of four dihydrobenzopyrazoloquinolines, (I)–(IV) (Figs. 1–4), synthesized by a simple solvent-free cyclocondensation, under microwave irradiation, of 5-amino-3-methyl-1-phenylpyrazole and the condensation products derived from 2-tetralone and a range of simple aldehydes. One objective of these structure determinations was the investigation of how the introduction of different simple aryl substituents at position 7 in compounds (II)–(IV) influences the supramolecular aggregation compared with that in the unsubstituted compound, (I). We have recently reported the

structures of the isomorphous and isostructural chlorophenyl and bromophenyl analogues, compounds (V) and (VI) (Serrano *et al.*, 2005*a,b*).



In each of compounds (I)–(IV), the bond distances within the fused heterocyclic components are consistent with aromatic delocalization within the pyridine ring, but with strong double-bond fixation in the C8—N9 bond of the pyrazole ring. The other distances and angles present no exceptional features. The non-aromatic carbocyclic ring adopts a nearly ideal screw-boat conformation (Evans & Boeyens, 1989) in each compound, as shown by the ring-puckering parameters (Cremer & Pople, 1975), given for the

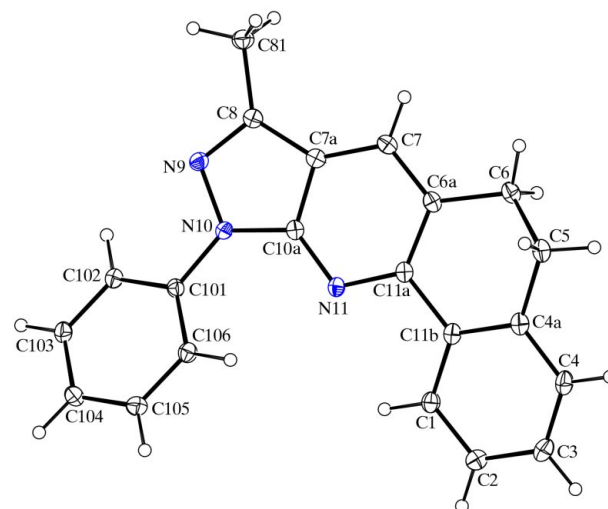


Figure 1
The molecule of (I), showing the atom-labelling scheme. Displacement ellipsoids are drawn at the 30% probability level.

atom sequence C4a—C5—C6—C6a—C11a—C11b in Table 1. For a six-membered ring with equal bond lengths throughout, the screw-boat conformation is characterized by $\theta = 67.5$ or 112.5° , and $\varphi = (60k + 30)^\circ$ ($k = \text{integer}$).

Associated with the screw-boat conformation of the non-aromatic carbocyclic ring, the two aromatic rings linked by the bond C11a—C11b (Figs. 1–4) are not parallel, and they make dihedral angles ranging from 11.11 (7°) in compound (III) to 15.78 (7°) in compound (II) (Table 1). The dihedral angles

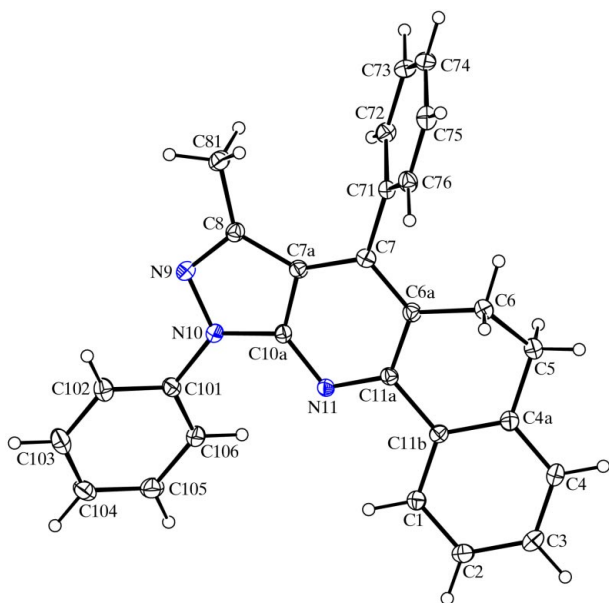


Figure 2
The molecule of (II), showing the atom-labelling scheme. Displacement ellipsoids are drawn at the 30% probability level.

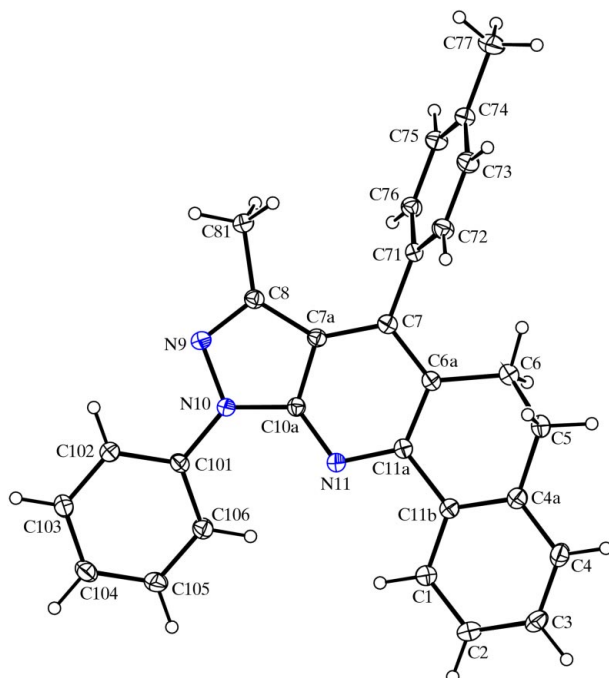


Figure 3
The molecule of (III), showing the atom-labelling scheme. Displacement ellipsoids are drawn at the 30% probability level.

between the pyridine ring and the pendent C71–C76 aryl ring are likewise very similar for compounds (II)–(IV). On the other hand, the dihedral angles between the pyrazole ring and the pendent C101–C106 aryl ring show a rather larger variation. It may be noted here that rings C71–C76 and C101–C106 participate in the hydrogen bonding in each of (II)–(IV), and that the hydrogen bonding may be an important factor in controlling these dihedral angles.

The supramolecular aggregation in compound (I) is extremely simple and involves just one hydrogen bond (Table 2). Atom C5 in the molecule at (x, y, z) acts as hydrogen-bond donor, *via* the axial atom H5A, to pyrazole atom N9 in the

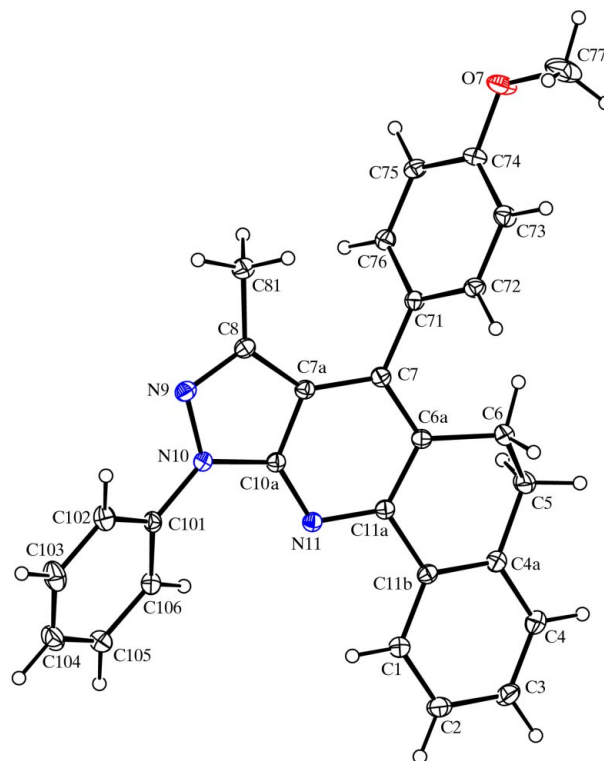


Figure 4
The molecule of (IV), showing the atom-labelling scheme. Displacement ellipsoids are drawn at the 30% probability level.

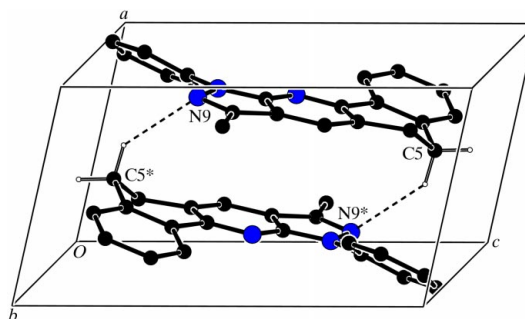


Figure 5
Part of the crystal structure of (I), showing the formation of a centrosymmetric hydrogen-bonded dimer. For the sake of clarity, H atoms bonded to those C atoms which are not involved in the motif shown have been omitted. Atoms marked with an asterisk (*) are at the symmetry position $(1 - x, 1 - y, 1 - z)$.

molecule at $(1-x, 1-y, 1-z)$, so forming a centrosymmetric $R_2^2(16)$ dimer centred at $(\frac{1}{2}, \frac{1}{2}, \frac{1}{2})$ (Fig. 5). The formation of this dimer is reinforced by a π - π stacking interaction involving the pyridine rings of the two component molecules. These rings are strictly parallel, with an interplanar spacing of 3.450 (2) Å. The ring-centroid separation is 3.729 (2) Å, corresponding to a nearly ideal ring offset of 1.415 (2) Å. There are no other direction-specific interactions between the molecules; in particular, C-H... π (arene) hydrogen bonds are absent. Hence, the structure of compound (I) simply consists of isolated centrosymmetric dimers.

By contrast with the structure of (I), there are no C-H...N hydrogen bonds in the structures of either (II) or (III). Instead, the molecules of (II) and (III) are linked into sheets by C-H... π (arene) hydrogen bonds, a type of interaction absent from the structure of (I). Despite crystallizing in the same space group, namely $P2_1/c$, the formation of the hydrogen-bonded sheets differs considerably between (II) and (III).

In compound (II), the pyridine ring and the pendent C101-C106 phenyl ring act as hydrogen-bond acceptors. In the shorter of the two hydrogen bonds (Table 2), atom C73 in the molecule at (x, y, z) acts as donor to the C101-C106 aryl ring in the molecule at $(1-x, 1-y, -z)$, so generating a cyclic

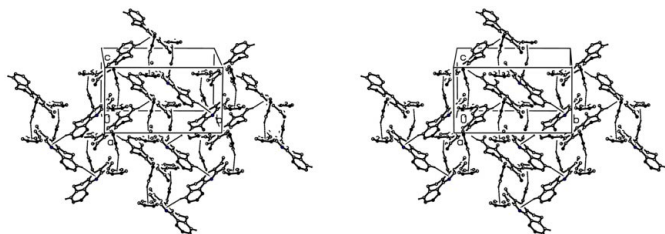


Figure 6
A stereoview of part of the crystal structure of (II), showing the formation of a hydrogen-bonded (100) sheet generated by the combination of an inversion and a glide plane. For the sake of clarity, H atoms not involved in the motifs shown have been omitted.

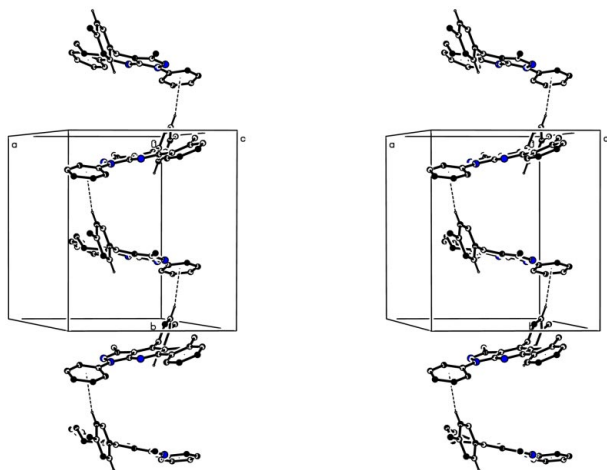


Figure 7
A stereoview of part of the crystal structure of (III), showing the formation of a hydrogen-bonded chain along [010] generated by a 2_1 screw axis. For the sake of clarity, H atoms not involved in the motif shown have been omitted.

and centrosymmetric dimeric motif centred at $(\frac{1}{2}, \frac{1}{2}, 0)$. The second of the two hydrogen bonds then links this dimer at $(\frac{1}{2}, \frac{1}{2}, 0)$ to four adjacent dimers. Atoms C4 in the molecules at (x, y, z) and $(1-x, 1-y, -z)$ act as hydrogen-bond donors to the pyridine rings in the molecules at $(x, \frac{1}{2}-y, \frac{1}{2}+z)$ and $(1-x, \frac{1}{2}+y, -\frac{1}{2}-z)$, respectively, which themselves form parts of the dimers centred at $(\frac{1}{2}, 0, \frac{1}{2})$ and $(\frac{1}{2}, 1, -\frac{1}{2})$, respectively. Similarly, the pyridine rings at (x, y, z) and $(1-x, 1-y, -z)$ accept hydrogen bonds from the C4 atoms in the molecules at $(x, \frac{1}{2}-y, z-\frac{1}{2})$ and $(1-x, \frac{1}{2}+y, \frac{1}{2}-z)$, which are themselves components of dimers centred at $(\frac{1}{2}, 0, -\frac{1}{2})$ and $(\frac{1}{2}, 1, \frac{1}{2})$. Propagation by the space group of these two hydrogen bonds, associated with an inversion and a c -glide plane, respectively, then generates a (100) sheet in which large and small rings alternate (Fig. 6).

As in (II), the two-dimensional supramolecular structure of (III) is built from two C-H... π (arene) hydrogen bonds (Table 2), but now both are associated with translational symmetry operations and there are no directly connected pairs

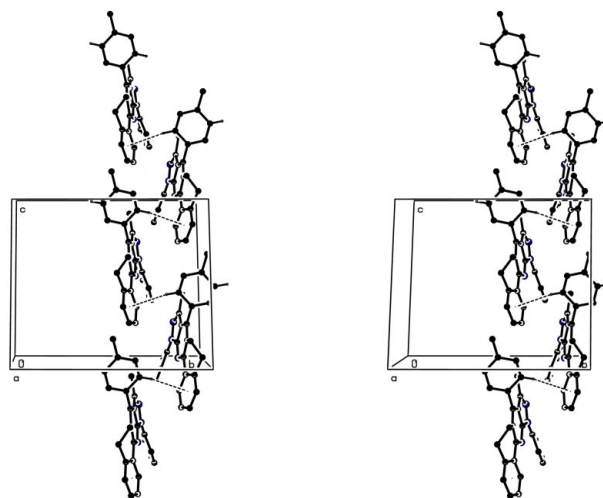


Figure 8
A stereoview of part of the crystal structure of (III), showing the formation of a hydrogen-bonded chain along [001] generated by a glide plane. For the sake of clarity, H atoms not involved in the motif shown have been omitted.

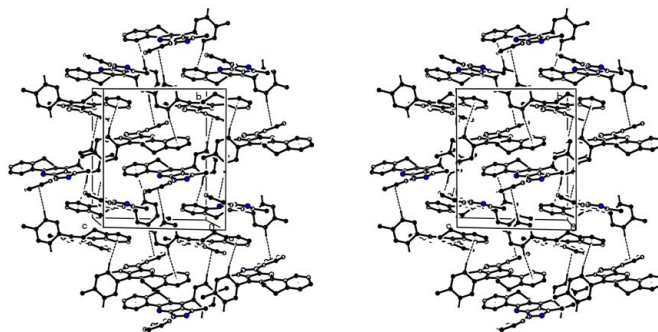


Figure 9
A stereoview of part of the crystal structure of (III), showing the formation of a hydrogen-bonded (100) sheet generated by the combination of the [010] and [001] chains. For the sake of clarity, H atoms not involved in the motifs shown have been omitted.

of molecules which are related by inversion. Again, unlike the hydrogen bonds in (II), for those in (III) the two donors form parts of the same aryl ring, while the acceptors are the two aryl rings pendent from the fused ring system.

Aryl atom C73 in the molecule at (x, y, z) acts as hydrogen-bond donor to the C101–C106 ring in the molecule at $(1 - x, y - \frac{1}{2}, \frac{3}{2} - z)$, thereby forming a chain running parallel to the [010] direction and generated by the 2_1 screw axis along $(\frac{1}{2}, y, \frac{3}{4})$ (Fig. 7). In addition, atom C76 at (x, y, z) acts as hydrogen-bond donor to the C1/C2/C3/C4/C4a/C11b ring in the molecule at $(x, \frac{3}{2} - y, \frac{1}{2} + z)$, thus producing a chain parallel to the [001] direction and generated by the c -glide plane at $y = \frac{3}{4}$ (Fig. 8). The combination of these two chains generates a (100) sheet in the form of a (4,4)-net (Fig. 9).

The constitution of compound (IV) differs from those of (I)–(III) in that it provides an additional acceptor of hydrogen

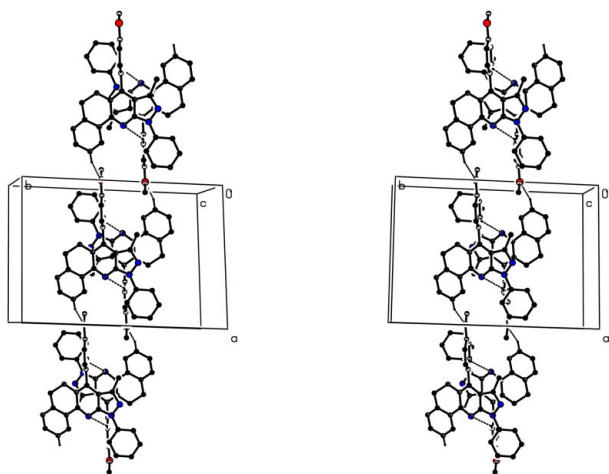


Figure 10

A stereoview of part of the crystal structure of (IV), showing the formation of a chain of edge-fused rings along [101] built from C–H...N and C–H...O hydrogen bonds. For the sake of clarity, H atoms not involved in the motif shown have been omitted.

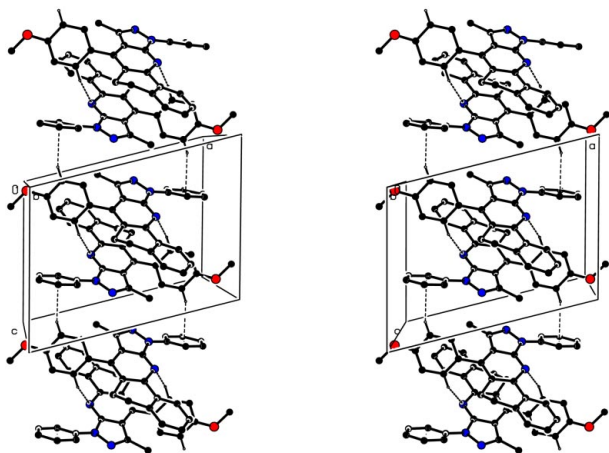


Figure 11

A stereoview of part of the crystal structure of (IV), showing the formation of a chain of edge-fused rings along [001] built from C–H...N and C–H... π (arene) hydrogen bonds. For the sake of clarity, H atoms not involved in the motif shown have been omitted.

bonds in the O atom of the methoxy substituent (Fig. 4). In fact, the molecules of (IV) are linked by a combination of C–H...N, C–H...O and C–H... π (arene) hydrogen bonds (Table 2) into a rather complex three-dimensional framework. The formation of this framework can be analysed very straightforwardly in terms of the component one-dimensional substructures.

In the first such substructure, the C–H...N and C–H...O hydrogen bonds combine to generate a chain of edge-fused rings. Aryl atom C72 in the molecule at (x, y, z) acts as hydrogen-bond donor to pyridine atom N11 in the molecule at $(1 - x, 1 - y, 1 - z)$, thereby generating a centrosymmetric $R_2^2(14)$ ring centred at $(\frac{1}{2}, \frac{1}{2}, \frac{1}{2})$. In addition, atom C2 at (x, y, z) acts as donor to atom O7 in the molecule at $(1 + x, y, 1 + z)$, so generating by translation a $C(12)$ chain running parallel to the [101] direction. The combination of these two hydrogen bonds then generates a chain of edge-fused rings, with $R_2^2(14)$ rings centred at $(n + \frac{1}{2}, \frac{1}{2}, n + \frac{1}{2})$ ($n = \text{zero or integer}$) and $R_4^4(22)$ rings centred at $(n, \frac{1}{2}, n)$ ($n = \text{zero or integer}$) (Fig. 10).

The second one-dimensional substructure also takes the form of a chain of edge-fused rings. Aryl atoms C75 in the molecules at (x, y, z) and $(1 - x, 1 - y, 1 - z)$, which form the $R_2^2(14)$ dimer centred at $(\frac{1}{2}, \frac{1}{2}, \frac{1}{2})$, act as hydrogen-bond donors to the C101–C106 rings in the molecules at $(1 - x, 1 - y, -z)$ and $(x, y, 1 + z)$, respectively, which themselves form part of the $R_2^2(14)$ dimers centred at $(\frac{1}{2}, \frac{1}{2}, -\frac{1}{2})$ and $(\frac{1}{2}, \frac{1}{2}, \frac{3}{2})$, respectively, so forming a chain of edge-fused centrosymmetric rings running parallel to the [001] direction (Fig. 11).

In addition to this [001] chain of edge-fused rings generated by inversion, there is a second substructure running parallel to [001] in the form of a simple chain generated by a c -glide plane. Aryl atom C4 in the molecule at (x, y, z) acts as hydrogen-bond donor to the pyridine ring in the molecule at $(x, \frac{3}{2} - y, \frac{1}{2} + z)$, producing an [001] chain generated by the c -glide plane at $y = \frac{3}{4}$ (Fig. 12).

In the final substructure, atom C103 in the molecule at (x, y, z) acts as hydrogen-bond donor to the pendent C71–C76 aryl

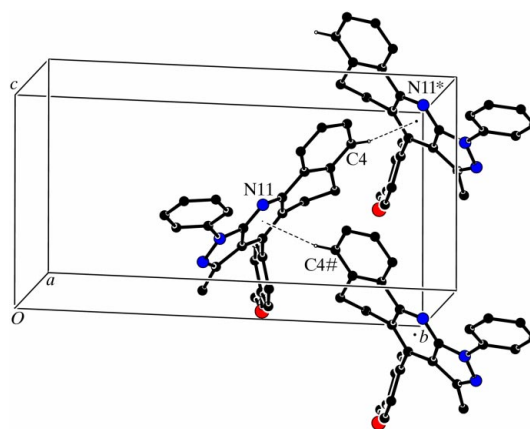


Figure 12

Part of the crystal structure of (IV), showing the formation of a simple [001] chain built from C–H... π (arene) hydrogen bonds. For the sake of clarity, H atoms not involved in the motif shown have been omitted. Atoms marked with an asterisk (*) or a hash (#) are at the symmetry positions $(x, \frac{3}{2} - y, \frac{1}{2} + z)$ and $(x, \frac{3}{2} - y, z - \frac{1}{2})$, respectively.

ring in the molecule at $(1-x, y - \frac{1}{2}, \frac{1}{2} - z)$, so forming a chain running parallel to the [010] direction and generated by the 2_1 screw axis along $(\frac{1}{2}, y, \frac{1}{4})$ (Fig. 13).

The combination of the chains along [010], [001] and [101] suffices to link all of the molecules into a single three-dimensional framework, the complexity of which arises largely from the occurrence in the structure of five independent hydrogen bonds (Table 2).

We briefly compare the supramolecular structures of compounds (I)–(IV) reported here with those of the pair of compounds, (V) and (VI) (see scheme), containing 4-halogenophenyl substituents, where the molecular skeleton is a simple positional isomer of the skeleton in compounds (I)–(IV), and which are themselves strictly isostructural in space group $P\bar{1}$, as reported recently (Serrano *et al.*, 2005*a,b*). In these analogues, the molecules are linked by $C-H \cdots \pi(\text{arene})$ hydrogen bonds into chains of edge-fused rings. Hence, within this rather compact group of compounds, *viz.* (I)–(VI), the supramolecular aggregation ranges from finite (zero-dimensional) in compound (I), *via* one-dimensional in compounds (V) and (VI) and two-dimensional in compounds (II) and (III), to three-dimensional in compound (IV).

The differences between the 4-methylphenyl compound, (III), and the 4-chlorophenyl compound, (V), in terms of both their space groups, namely $P2_1/c$ for (III) as opposed to $P\bar{1}$ for (V), and their supramolecular dimensionality, namely two-dimensional for (III) as opposed to one-dimensional for (V), is

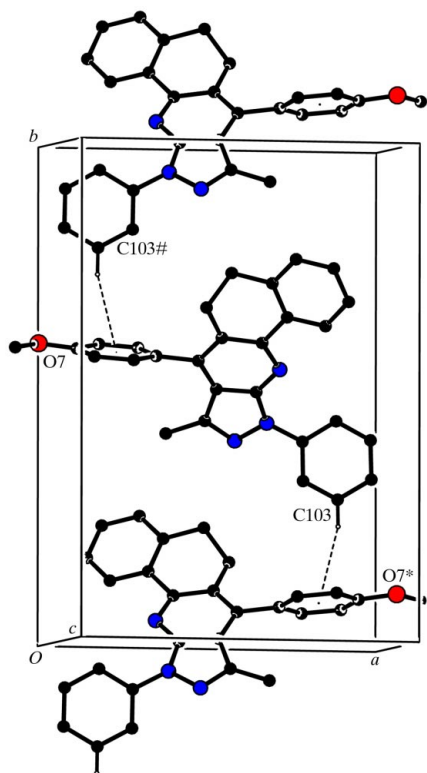


Figure 13

Part of the crystal structure of (IV), showing the formation of a simple [010] chain built from $C-H \cdots \pi(\text{arene})$ hydrogen bonds. For the sake of clarity, H atoms not involved in the motif shown have been omitted. Atoms marked with an asterisk (*) or a hash (#) are at the symmetry positions $(1-x, y - \frac{1}{2}, \frac{1}{2} - z)$ and $(1-x, \frac{1}{2} + y, \frac{1}{2} - z)$, respectively.

unexpected, as methyl and chloro substituents on aryl rings are generally effectively isosteric. This is well illustrated, for example, by the related series of fused heterocycles (VII)–(IX) (see scheme) containing, respectively, 4-methylphenyl, 4-chlorophenyl and 4-bromophenyl substituents, which are all isomorphous and strictly isostructural (Portilla *et al.*, 2005).

Experimental

For the preparation of the title compounds, equimolar quantities of 5-amino-3-methyl-1-phenylpyrazole (1.0 mmol) and the corresponding methylene derivative (from 2-tetralone and the appropriate aldehyde) (1.0 mmol) were placed in open Pyrex glass vessels and irradiated in a domestic microwave oven for 3–5 min at 600 W. The reaction mixture was extracted with ethanol and the extract was evaporated. The solid residues were recrystallized from dimethylformamide to give crystals suitable for single-crystal X-ray diffraction. Analysis for (I): yellow crystals (m.p. 439–440 K, yield 60%), MS (30 eV) m/z (%) = 311 (100, M^+), 296 (7); for (II): yellow crystals (m.p. 494–495 K, yield 78%), MS (30 eV) m/z (%) = 388 (36), 387 (100, M^+), 372 (6); for (III): yellow crystals (m.p. 484–485 K, yield 75%), MS (30 eV) m/z (%) = 402 (36), 401 (100, M^+), 386 (6); for (IV): pale-brown crystals (m.p. 484–485 K, yield 60%), MS (30 eV) m/z (%) = 418 (33), 417 (100, M^+), 402 (6).

Compound (I)

Crystal data

$C_{21}H_{17}N_3$
 $M_r = 311.38$
 Triclinic, $P\bar{1}$
 $a = 7.0870$ (2) Å
 $b = 10.1321$ (4) Å
 $c = 11.7977$ (5) Å
 $\alpha = 87.501$ (2)°
 $\beta = 73.171$ (3)°
 $\gamma = 74.828$ (2)°
 $V = 782.13$ (5) Å³

$Z = 2$
 $D_x = 1.322$ Mg m⁻³
 Mo $K\alpha$ radiation
 Cell parameters from 3576 reflections
 $\theta = 3.1$ – 27.6 °
 $\mu = 0.08$ mm⁻¹
 $T = 120$ (2) K
 Rod, yellow
 $0.50 \times 0.10 \times 0.10$ mm

Data collection

Bruker–Nonius KappaCCD area-detector diffractometer
 φ and ω scans
 Absorption correction: multi-scan (SADABS; Sheldrick, 2003)
 $T_{\min} = 0.954$, $T_{\max} = 0.992$
 15116 measured reflections

3576 independent reflections
 2810 reflections with $I > 2\sigma(I)$
 $R_{\text{int}} = 0.039$
 $\theta_{\max} = 27.6$ °
 $h = -8 \rightarrow 9$
 $k = -12 \rightarrow 13$
 $l = -15 \rightarrow 15$

Refinement

Refinement on F^2
 $R[F^2 > 2\sigma(F^2)] = 0.043$
 $wR(F^2) = 0.114$
 $S = 1.04$
 3576 reflections
 218 parameters
 H-atom parameters constrained

$w = 1/[\sigma^2(F_o^2) + (0.0601P)^2 + 0.1501P]$
 where $P = (F_o^2 + 2F_c^2)/3$
 $(\Delta/\sigma)_{\max} < 0.001$
 $\Delta\rho_{\max} = 0.23$ e Å⁻³
 $\Delta\rho_{\min} = -0.28$ e Å⁻³

Compound (II)

Crystal data

$C_{27}H_{21}N_3$
 $M_r = 387.47$
 Monoclinic, $P2_1/c$
 $a = 11.5561$ (4) Å
 $b = 17.6751$ (7) Å
 $c = 9.8469$ (3) Å
 $\beta = 98.599$ (2)°
 $V = 1988.67$ (12) Å³
 $Z = 4$

$D_x = 1.294$ Mg m⁻³
 Mo $K\alpha$ radiation
 Cell parameters from 4539 reflections
 $\theta = 2.9$ – 27.5 °
 $\mu = 0.08$ mm⁻¹
 $T = 120$ (2) K
 Block, yellow
 $0.40 \times 0.20 \times 0.20$ mm

Data collection

Bruker–Nonius KappaCCD area-detector diffractometer
 φ and ω scans
 Absorption correction: multi-scan (SADABS; Sheldrick, 2003)
 $T_{\min} = 0.973$, $T_{\max} = 0.985$
 26788 measured reflections

4539 independent reflections
 3236 reflections with $I > 2\sigma(I)$
 $R_{\text{int}} = 0.053$
 $\theta_{\text{max}} = 27.5^\circ$
 $h = -15 \rightarrow 13$
 $k = -22 \rightarrow 22$
 $l = -12 \rightarrow 12$

Refinement

Refinement on F^2
 $R[F^2 > 2\sigma(F^2)] = 0.048$
 $wR(F^2) = 0.126$
 $S = 1.08$
 4539 reflections
 272 parameters
 H-atom parameters constrained

$w = 1/[\sigma^2(F_o^2) + (0.0639P)^2 + 0.3388P]$
 where $P = (F_o^2 + 2F_c^2)/3$
 $(\Delta/\sigma)_{\text{max}} < 0.001$
 $\Delta\rho_{\text{max}} = 0.28 \text{ e } \text{Å}^{-3}$
 $\Delta\rho_{\text{min}} = -0.29 \text{ e } \text{Å}^{-3}$

Compound (III)

Crystal data

$\text{C}_{28}\text{H}_{23}\text{N}_3$
 $M_r = 401.49$
 Monoclinic, $P2_1/c$
 $a = 12.0313 (3) \text{ Å}$
 $b = 14.3347 (4) \text{ Å}$
 $c = 12.7956 (3) \text{ Å}$
 $\beta = 109.3092 (14)^\circ$
 $V = 2082.66 (9) \text{ Å}^3$
 $Z = 4$

$D_x = 1.280 \text{ Mg m}^{-3}$
 Mo $K\alpha$ radiation
 Cell parameters from 4778 reflections
 $\theta = 3.2\text{--}27.5^\circ$
 $\mu = 0.08 \text{ mm}^{-1}$
 $T = 120 (2) \text{ K}$
 Lath, yellow
 $0.66 \times 0.42 \times 0.14 \text{ mm}$

Data collection

Bruker–Nonius KappaCCD area-detector diffractometer
 φ and ω scans
 Absorption correction: multi-scan (SADABS; Sheldrick, 2003)
 $T_{\min} = 0.956$, $T_{\max} = 0.989$
 38247 measured reflections

4778 independent reflections
 3416 reflections with $I > 2\sigma(I)$
 $R_{\text{int}} = 0.059$
 $\theta_{\text{max}} = 27.5^\circ$
 $h = -15 \rightarrow 15$
 $k = -18 \rightarrow 18$
 $l = -16 \rightarrow 16$

Refinement

Refinement on F^2
 $R[F^2 > 2\sigma(F^2)] = 0.050$
 $wR(F^2) = 0.129$
 $S = 1.04$
 4778 reflections
 282 parameters
 H-atom parameters constrained

$w = 1/[\sigma^2(F_o^2) + (0.066P)^2 + 0.5056P]$
 where $P = (F_o^2 + 2F_c^2)/3$
 $(\Delta/\sigma)_{\text{max}} < 0.001$
 $\Delta\rho_{\text{max}} = 0.41 \text{ e } \text{Å}^{-3}$
 $\Delta\rho_{\text{min}} = -0.31 \text{ e } \text{Å}^{-3}$

Compound (IV)

Crystal data

$\text{C}_{28}\text{H}_{23}\text{N}_3\text{O}$
 $M_r = 417.49$
 Monoclinic, $P2_1/c$
 $a = 12.9148 (3) \text{ Å}$
 $b = 17.5938 (5) \text{ Å}$
 $c = 9.8192 (2) \text{ Å}$
 $\beta = 104.3370 (17)^\circ$
 $V = 2161.64 (9) \text{ Å}^3$
 $Z = 4$

$D_x = 1.283 \text{ Mg m}^{-3}$
 Mo $K\alpha$ radiation
 Cell parameters from 4963 reflections
 $\theta = 3.3\text{--}27.5^\circ$
 $\mu = 0.08 \text{ mm}^{-1}$
 $T = 120 (2) \text{ K}$
 Plate, pale brown
 $0.50 \times 0.20 \times 0.05 \text{ mm}$

Data collection

Bruker–Nonius KappaCCD area-detector diffractometer
 φ and ω scans
 Absorption correction: multi-scan (SADABS; Sheldrick, 2003)
 $T_{\min} = 0.974$, $T_{\max} = 0.996$
 35681 measured reflections

4963 independent reflections
 3449 reflections with $I > 2\sigma(I)$
 $R_{\text{int}} = 0.062$
 $\theta_{\text{max}} = 27.5^\circ$
 $h = -16 \rightarrow 16$
 $k = -22 \rightarrow 22$
 $l = -12 \rightarrow 11$

Refinement

Refinement on F^2
 $R[F^2 > 2\sigma(F^2)] = 0.044$
 $wR(F^2) = 0.112$
 $S = 1.04$
 4963 reflections
 291 parameters
 H-atom parameters constrained

$w = 1/[\sigma^2(F_o^2) + (0.0534P)^2 + 0.4296P]$
 where $P = (F_o^2 + 2F_c^2)/3$
 $(\Delta/\sigma)_{\text{max}} = 0.001$
 $\Delta\rho_{\text{max}} = 0.21 \text{ e } \text{Å}^{-3}$
 $\Delta\rho_{\text{min}} = -0.27 \text{ e } \text{Å}^{-3}$

Table 1

Ring-puckering parameters and selected dihedral angles (Å , $^\circ$) for compounds (I)–(IV).

The ring-puckering parameters for the non-aromatic carbocyclic ring are calculated for the atom sequence C4a–C5–C6–C6a–C11a–C11b.

Parameter	(I)	(II)	(III)	(IV)
Q	0.423 (2)	0.461 (2)	0.460 (2)	0.450 (2)
θ	63.9 (2)	115.4 (2)	61.5 (2)	115.5 (2)
φ	89.6 (2)	274.1 (2)	96.6 (2)	271.6 (2)
(C1–C4/C4a/C11b)/pyridine	13.84 (7)	15.78 (7)	11.11 (7)	14.79 (7)
(C71–C76)/pyridine		63.45 (7)	65.27 (7)	60.88 (7)
(C101–C106)/pyrazole	26.21 (7)	33.16 (8)	18.56 (8)	30.30 (4)

Table 2

Hydrogen-bond geometry (Å , $^\circ$) for compounds (I)–(IV).

Cg1–Cg4 are the centroids of rings N11/C10a/C7a/C7/C6a/C11a, C101–C106, C1–C4/C4a/C11a and C71–C76, respectively.

	D–H...A	D–H	H...A	D...A	D–H...A
(I)	C5–H5A...N9 ⁱ	0.99	2.60	3.4070 (18)	139
(II)	C4–H4...Cg1 ⁱⁱ	0.95	2.82	3.7461 (17)	164
	C73–H73...Cg2 ⁱⁱⁱ	0.95	2.62	3.4852 (17)	152
(III)	C73–H73...Cg2 ^{iv}	0.95	2.96	3.8991 (18)	168
	C76–H76...Cg3 ^v	0.95	2.90	3.8349 (17)	168
(IV)	C2–H2...O7 ^{vi}	0.95	2.53	3.3422 (18)	144
	C72–H72...N11 ⁱ	0.95	2.60	3.3952 (17)	142
	C4–H4...Cg1 ^v	0.95	2.84	3.7766 (17)	168
	C75–H75...Cg2 ⁱⁱⁱ	0.95	2.67	3.5605 (15)	157
	C103–H103...Cg4 ^{vii}	0.95	2.85	3.7417 (19)	157

Symmetry codes: (i) $1-x, 1-y, 1-z$; (ii) $x, \frac{1}{2}-y, \frac{1}{2}+z$; (iii) $1-x, 1-y, -z$; (iv) $1-x, y-\frac{1}{2}, \frac{3}{2}-z$; (v) $x, \frac{3}{2}-y, \frac{1}{2}+z$; (vi) $1+x, y, 1+z$; (vii) $1-x, y-\frac{1}{2}, \frac{1}{2}-z$.

Crystals of compound (I) are triclinic; space group $P\bar{1}$ was selected and then confirmed by the successful structure analysis. For each of compounds (II)–(IV), the space group $P2_1/c$ was uniquely assigned from the systematic absences. All H atoms were located from difference maps and then treated as riding atoms, with C–H distances of 0.95 (aromatic), 0.98 (CH₃) or 0.99 Å (CH₂), and with $U_{\text{iso}}(\text{H}) = 1.2U_{\text{eq}}(\text{C})$, or $1.5U_{\text{eq}}(\text{C})$ for the methyl groups. The crystals of compound (III) were very fragile, and attempts to cut small fragments from larger crystals resulted in shattering.

For all compounds, data collection: COLLECT (Hoof, 1999); cell refinement: DENZO (Otwinowski & Minor, 1997) and COLLECT; data reduction: DENZO and COLLECT; program(s) used to solve structure: OSCAIL (McArdle, 2003) and SHELXS97 (Sheldrick, 1997); program(s) used to refine structure: OSCAIL and SHELXL97 (Sheldrick, 1997); molecular graphics: PLATON (Spek, 2003); software used to prepare material for publication: SHELXL97 and PRPKAPPA (Ferguson, 1999).

The X-ray data were collected at the EPSRC X-ray Crystallographic Service, University of Southampton. JC thanks the Consejería de Innovación, Ciencia y Empresa (Junta de

Andalucía, Spain) and the Universidad de Jaén for financial support. JQ and JP thank COLCIENCIAS and UNIVALLE (Universidad del Valle, Colombia) for financial support.

Supplementary data for this paper are available from the IUCr electronic archives (Reference: SK1854). Services for accessing these data are described at the back of the journal.

References

- Cremer, D. & Pople, J. A. (1975). *J. Am. Chem. Soc.* **97**, 1354–1358.
- Evans, D. G. & Boeyens, J. C. A. (1989). *Acta Cryst.* **B45**, 581–590.
- Ferguson, G. (1999). *PRPKAPPA*. University of Guelph, Canada.
- Hooft, R. W. W. (1999). *COLLECT*. Nonius BV, Delft, The Netherlands.
- McArdle, P. (2003). *OSCAIL for Windows*. Version 10. Crystallography Centre, Chemistry Department, NUI Galway, Ireland.
- Otwinowski, Z. & Minor, W. (1997). *Methods in Enzymology*, Vol. 276, *Macromolecular Crystallography*, Part A, edited by C. W. Carter Jr & R. M. Sweet, pp. 307–326. New York: Academic Press.
- Portilla, J., Quiroga, J., Cobo, J., Low, J. N. & Glidewell, C. (2005). *Acta Cryst.* **C61**, o452–o456.
- Quiroga, J., Mejía, D., Insuasty, B., Abonia, R., Noguerras, M., Sánchez, A., Cobo, J. & Low, J. N. (2001). *Tetrahedron*, **57**, 6947–6953.
- Serrano, H., Quiroga, J., Cobo, J., Low, J. N. & Glidewell, C. (2005a). *Acta Cryst.* **E61**, o1058–o1060.
- Serrano, H., Quiroga, J., Cobo, J., Low, J. N. & Glidewell, C. (2005b). *Acta Cryst.* **E61**, o1702–o1703.
- Sheldrick, G. M. (1997). *SHELXS97* and *SHELXL97*. University of Göttingen, Germany.
- Sheldrick, G. M. (2003). *SADABS*. Version 2.10. University of Göttingen, Germany.
- Spek, A. L. (2003). *J. Appl. Cryst.* **36**, 7–13.